RESEARCH ARTICLE
Journal of Biometry Studies (2022) 2(2): 78-86
DOI: 10.29329/JofBS.2022.445.05
www.biometrystudies.com

Journal of Biometry Studies
PRENSİP
www.prensip.gen.tr

Estimation of aboveground carbon storage based on remote sensing and inventory data: A case study from Türkiye

Fatih SİVRİKAYA[1,*], Döndü DEMİEL[1]

[1]Kastamonu University, Faculty of Forestry, Department of Forest Management, Kastamonu/TURKIYE

[*]Corresponding author: fsivrikaya@kastamonu.edu.tr

Received: 21/12/2022, Accepted: 28/12/2022

Abstract

Forest ecosystems are one of the most important systems in capturing atmospheric carbon dioxide (CO_2) and play an essential role in mitigating climate change. Forest ecosystems provide biodiversity, soil conservation, recreation areas, wildlife habitat, nutrient cycling, carbon storage and oxygen production. According to the Climate Change Framework Convention, determining and reporting the amount of carbon accumulation in forest ecosystem is of great importance. Different methods such as allometric equations, carbon expansion factor and remote sensing methods are used to determine aboveground carbon (AGC) storage. Especially with the developing technology, remote sensing techniques are used intensively to determine AGC storage. Normalized Difference Vegetation Index (NDVI) are commonly used, especially in determining the amount of AGC storage. The aim of this study is to estimate AGC storage according to different methods and to investigate whether there are statistical differences in AGC storage estimation of these approaches. The research was carried out in pure Calabrian pine (*Pinus brutia* Ten.) stands in the Burmahanyayla planning unit in Antalya province in the Mediterranean region of Türkiye. Within the scope of the study, the amount of AGC storage was calculated by using the inventory study conducted in 2022 and the Landsat 9 satellite data. A paired sample t-test was used to statistically examine the difference in the quantity of AGC storage based on inventory data and remote sensing data using SPSS 23.0. The results reveal that there was no statistically significant difference in the AGC storage values between the two approaches in all sample plots.

Keywords: Allometric equations, Aboveground carbon storage, NDVI, Remote sensing

Please cite this article as follows:
Sivrikaya, F., & Demirel, D. (2022). Estimation of Aboveground Carbon Storage Based on Remote Sensing and Inventory Data: A Case Study from Türkiye. *Journal of Biometry Studies*, *2*(2), 78-86. https://doi.org/10.29329/JofBS.2022.445.05

1. Introduction

With the economic, ecological and socio-cultural changes in the world, carbon dioxide (CO_2) emissions are also increasing. CO_2 emissions are especially affected by the increasing population, industrialization, and the use of fossil fuels. One of the most dangerous greenhouse gases is CO_2 (Lal, 2008). Global climate change is a reality that we face as a result of increasing carbon dioxide emissions. The most effective fight against global climate change is to reduce greenhouse gas emissions and increase the amount of carbon held in the atmosphere (Sakici et al., 2018). Forests are one of the most important system in reducing carbon dioxide emissions in the atmosphere and creating carbon pools (Çepel, 2003). 82% of the carbon in the terrestrial ecosystem is stored in forest ecosystems (Cusack et al., 2014; Kauranne et al., 2017). In addition, 80% of aboveground carbon and 40% of underground carbon are stored in forest ecosystems (Goodale et al., 2002; Turgut & Günlü, 2022). Therefore, determining the amount of carbon storage in forests has an essential part of the global carbon cycle for greenhouse gas emissions. The amount of carbon stored in the forests of Türkiye is obtained from forest management plans.

The amount of biomass and carbon storage is calculated with the help of allometric equations and biomass expansion factors (BEF) (Wharton & Griffith, 1993; Sivrikaya et al., 2007; Sivrikaya & Işık, 2022). The variables related to these methods are inventory data

(Sivrikaya et al., 2013; Sakici et al., 2018; Sağlam et al., 2020; Güner et al., 2022) and remote sensing data (Günlü et al., 2014; Chen et al., 2018; Anand et al., 2020; Günlü & Ercanlı, 2020; Keleş et al., 2021; Perry et al., 2022; Turgut & Günlü, 2022; Bulut et al., 2022). In order to determine the amount of carbon stored in the forest ecosystem with inventory data, first of all, biomass is determined (Sivrikaya & Bozali, 2012). This method is expensive, labor-intensive and time-consuming. However, with remote sensing data, the amount of carbon can be determined with less cost and labor in larger areas. Band values (Gou et al., 2022; Wallis et al., 2023), vegetation indices (Li et al., 2018; Chen et al., 2018; Nurda et al., 2020; Wang et al., 2020; Gardin et al., 2021; Perry et al., 2022; Dvorakova et al., 2023) and texture values (Chen et al., 2018; Günlü et al., 2021; Keleş et al., 2022) are used to determine the amount of carbon by remote sensing. NDVI (Normalized Difference Vegetation Index) data obtained from satellite images such as Landsat, Sentinel-1, Sentinel-2 and Lidar are widely used to reveal the relationships between the amount of carbon storage (Myeong et al., 2006; Baniya et al., 2018; Xiao et al.,2019; Dvorakova et al., 2020; Wang et al., 2021; Keleş et al., 2021; Dvorakova et al., 2023).

In this study, it is aimed to determine the aboveground carbon (AGC) storage with the NDVI data acquired from the Landsat 9 satellite image, as an alternative to expensive, labor-intensive applications. In addition, the amount of AGC storage was determined by using the forest inventory data of the study area using allometric equation. The relationships between AGC storage estimated according to both forest inventory and remote sensing data were investigated using regression analysis.

2. Material and Methods

2.1. Study area

The Burmahanyayla planning unit (PU) was selected as a case study area, located in Antalya Regional Directorate of Forestry in Türkiye. The study area is situated in the south of Türkiye, Mediterranean region, at 36° 49′–37° 26′ N and 31° 08′–31° 24′ E (Figure 1). The Burmahanyayla PU covers a total area of 21364.9 hectares, of which 9014.9 hectares are productive forest and 2990.4 hectares are degraded forest (FMP, 2022). Calabrian pine (*Pinus brutia* Ten.), Crimean pine (*Pinus nigra* J.F.Arnold), Cedar (*Cedrus libani* A. Rich.), and Juniper (*Juniperus* ssp.) are the main tree species in the study area. The research region is under zone *Csa* of the Köppen climate classification system, characterized by a hot summer. In this region, at least one month's average temperature is over 22 °C, the coldest month averages above 0 °C, and at least four months have average temperatures that are above 10 °C. The wettest month of the year has at least three times as much precipitation as the driest month of the year, which only receives 40 mm or less (Beck et al., 2018).

2.2. Forest inventory data

General Directorate of Forestry in Türkiye is largely responsible for creating forest management plans. In every ten or twenty years, forest management plans are updated. The initial stage of the planning procedure is the forest inventory, based on both field survey and remotely sensed data (satellite image classification or aerial picture interpretation). Türkiye's Forest Management Team (FMT) conducts forest inventories. Forest inventory study was carried out in 2022 in order to renew the forest management plans in the Burmahanyayla PU. Sample plots were created systematically at 300x300 meters intervals and a total of 228 sample plots were taken from pure Calabrian pine stands within the scope of the field study. Sample plots were collected in the shape of a circle and their dimensions were taken as 400 m^2 (crown closure >70%), 600 m^2 (crown closure >40-70) and 800 m^2 (crown closure >11-40%). The GPS was used to find the locations of each sample plot. In each sample plot, the diameters of all trees with a diameter at breast height (*dbh*, cm) larger than 7.9 cm were measured.

2.3. Data processing for Landsat satellite image

The Landsat 9 satellite, which have the same orbit with the Landsat 8 satellite, was launched on September 27, 2021. Landsat 9 has a temporal resolution of 8 days and a radiometric resolution of 14 bits. Having more radiometric resolution than Landsat 8 will provide a better perception of ecosystems with complex structures such as forests. The Landsat 9 satellite image includes 11 spectral bands, including near-short wave infrared and thermal infrared spectral bands. Within the scope of the study, Landsat 9 satellite image was downloaded free of charge from http://earthexplorer.usgs.gov in Level-1 format (Table 1). Red and Near-Infrared bands (Band 4 and Band 5) of the Landsat 9 satellite image were used in this study. The satellite image was geo-referenced with the root means square error (RMSE) less than one pixel to a Universal Transverse Mercator (UTM) coordinate system. The satellite image was subjected to some preprocessing such as geometric correction, atmospheric correction and calibration. It was clipped according to the boundaries of the study area and made ready for analysis. The GPS locations do, however contain positional inaccuracies, which typically average 4 m. As a result, it is almost impossible to find each sample plot and test point precisely in the middle of the 30 m grid of Landsat 9. Due of this, several studies used a window, such as a 3x3 pixel, to tackle the location problem (Labrecque et al. 2006; Turgut & Günlü, 2022). Reflectance values were averaged over the surrounding pixels using a window. In each example figure, the average of the NDVI values of nine pixels were calculated using a 3x3 window using ArcGIS 10.6 with Equation 1.

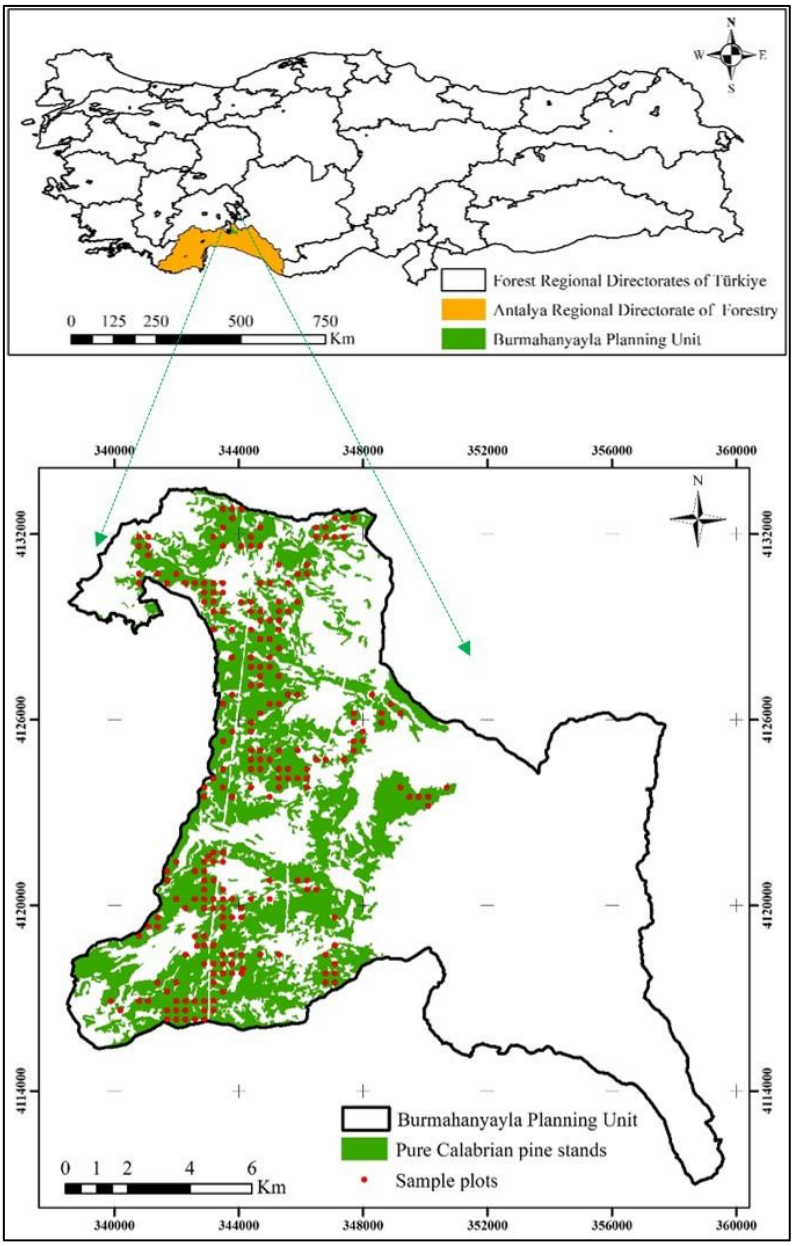

Figure 1. The case study area

Table 1. The properties of Landsat 9 images used in the study

Acquisition Date	Cloud cover (%)	Band Name	Central wavelength (μm)	Spatial resolution (m)
17.07.2022	4.58	Band 1 Ultra blue	0.43 - 0.45	30
		Band 2 Blue	0.45 - 0.51	30
		Band 3 Green	0.53 - 0.59	30
		Band 4 Red	0.64 - 0.67	30
		Band 5 Near-Infrared	0.85 - 0.88	30
		Band 6 SWIR	1.57 - 1.65	30
		Band 7 SWIR	2.11 - 2.29	30
		Band 8 Panchromatic	0.50 - 0.68	15
		Band 9 Cirrus	1.36 - 1.38	30
		Band 10 TIRS 1	10.6 - 11.19	100
		Band 11 TIRS 2	11.5 - 12.51	100

$$NDVI = \frac{NIR - Red}{NIR + Red} \quad (1)$$

where *NDVI* is Normalized Vegetation Index, *NIR* is the near infrared wavelength of the spectrum (0.85 – 0.88 μm), and *Red* is the red region wavelength (0.64 – 0.67 μm).

NDVI ranges from -1 to +1. As NDVI values approach +1 value, green vegetation increases and an NDVI value close to 0 means that the area has openness or low vegetation. In the case of water, snow and cloudiness in the satellite image, the NDVI value is close to -1.

2.4. Aboveground carbon storage estimation

For each sample plot, the AGC storage of each tree was determined using the following Equation (2) derived by Kahriman et al. (2016) for pure Calabrian pine forests. The sum of the AGC storage of the trees in each sample plot was used to get the total AGC storage. The AGC storage per hectare was then calculated.

$$\ln Y = -3{,}1961 + \frac{2{,}4596}{dbh} - 2{,}3796 \ln \frac{1}{dbh} \quad (2)$$

where *Y* is aboveground carbon (AGC) storage (ton), *dbh* is the diameter at breast height (cm).

First of all, correlation analysis was performed between AGC storage and NDVI values for each sample area using the Pearson correlation test. The simple linear regression analysis was performed to model the relationships between AGC storage and NDVI values acquired from Landsat 9 satellite image. The Paired sample *t*-test was used to determine whether there was a statistically difference between the AGC storage obtained from inventory data and AGC storage obtained from the NDVI data. All analysis was carried out using SPSS version 23.0.

3. Results and Discussion

In the forest inventory, *dbh* was measured in 4912 trees in 228 sample plots. It was between 8 cm and 100 cm, with an average of 26 cm. The NDVI values of the sample plots varied between 0.15 and 0.38. The mean NDVI value was calculated as 0.27. The AGC storage was calculated using carbon equation developed by Kahriman et al. (2016). The average AGC storage per hectare in the sample plots was 54.62 tons ha^{-1}, and the AGC storage varied between 3.58 tons ha^{-1} and 141.66 tons ha^{-1}. According to the AGC storage developed with NDVI values, the average AGC storage per hectare was estimated as 52.62 tons ha^{-1}, minimum 9.47 tons ha^{-1}, and the highest 176.03 tons ha^{-1} (Table 2).

The relationships between the NDVI values acquired from the Landsat 9 satellite image and the AGC storage estimated using inventory data for each sample plots were determined by correlation analysis. Correlation analysis showed a significant relationship between AGC storage and NDVI values (p<0.05). A high positive correlation was found between AGC storage and NDVI (r=0.779). These relationships between NDVI and AGC storage were modeled by regression analysis. Regression analysis showed exponential relationships between NDVI values and AGC storage, and it was determined that AGC storage increased with increasing NDVI value (Figure 2). The regression equation (Equation 3) was developed (R^2=0.623) to estimate the AGC storage with NDVI. With this developed equation, the AGC storage was estimated with 62% accuracy. Exponential regression equation;

$$AGC\ Storage\ (ton/ha) = 1.4317 * e^{(12.76333 * NDVI)} \quad (3)$$

The statistical validity of the model developed for AGC storage using NDVI values obtained from Landsat 9 satellite imagery was tested with a paired t-test at 95% confidence level. There was no statistically significant difference between AGC storage calculated according to both NDVI data and inventory data (p>0.05). As a result, the model developed to predict AGC storage with NDVI was found to be statistically appropriate. The NDVI value with the highest area (9918 ha) in the planning unit is between 0.20-0.30. NDVI value with the lowest area (287 ha) is less than 0.10 (Table 3). The NDVI map of the case study area was given in Figure 3.

According to the model developed using the NDVI values, the AGC storage amount per hectare of the planning unit was calculated. According to the results, the AGC storage per hectare of 62% of the planning unit (13272 ha) was less than 40 tons. The amount of AGC storage per hectare greater than 120 tons is only 697 ha (3% of the study area) (Table 4). This shows that there were more young stands in the study area. The AGC storage map of the model developed with NDVI values was given in Figure 4.

Table 2. Descriptive statistics of the sample plots

	dbh (cm)	NDVI	AGC storage using inventory data (tons ha^{-1})	AGC storage using NDVI (tons ha^{-1})
Minimum	8	0.15	3.58	9.47
Maximum	100	0.38	141.66	176.03
Mean	26	0.27	54.62	52.62
Standard Deviation	14.27	0.04	26.97	26.67
Variance	203.624	0.001	727.28	711.218

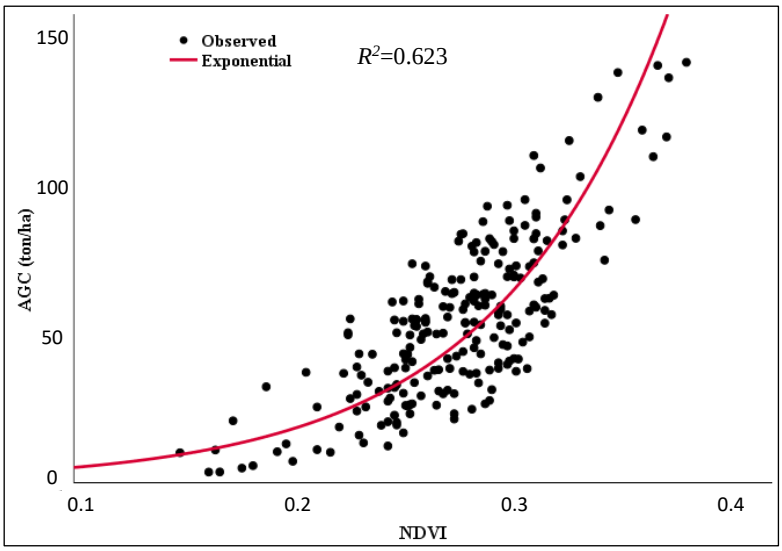

Figure 2. Relationship between NDVI values and AGC storage

Table 3. Distribution of NDVI value in the case study area

NDVI value	Area (ha)	Percentage (%)
<0.10	286.89	1.34
0.10 – 0.20	7445.38	34.85
0.20 – 0.30	9918.14	46.42
>0.30	3714.49	17.39
Total	21364.90	100.00

Table 4. Distribution of AGC storage in the study area

AGC Storage (ton)	Area (ha)	Percentage (%)
<40	13272.38	62.12
40 – 80	5769.68	27.01
80 – 120	1625.56	7.61
>120	697.28	3.26
Total	21364.90	100.00

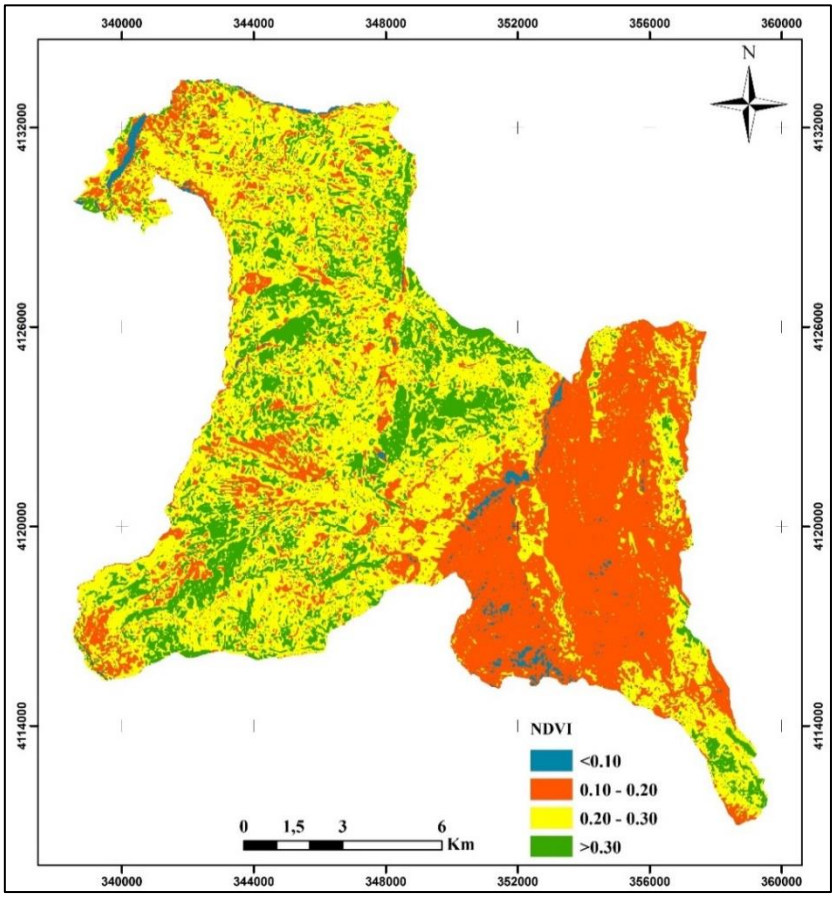

Figure 3. NDVI map of the case study area

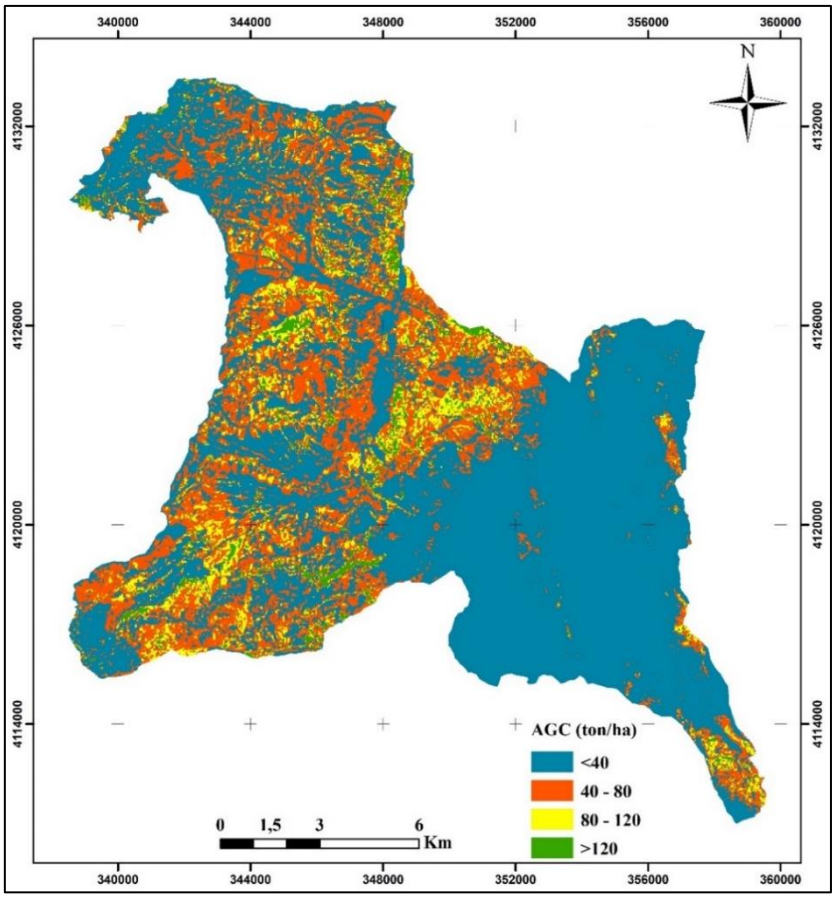

Figure 4. AGC storage map obtained with the model developed using NDVI in the case study area

Pungpa et al. (2023) used Landsat 5 TM and Landsat 9 OLI satellite imagery to estimate carbon storage and biomass. NDVI, SAVI, GNDVI and EXG indices were calculated from satellite images. The R^2 values of all models developed were found to be very close to zero (0.01-0.05). Among these models, the R^2 value of the model developed with NDVI values was found to be 0.05. Jiang et al. (2022) estimated carbon storage using Landsat 8 and Landsat 9 satellite imageries. Coefficients of models (R^2) were found to be 0.88 and 0.87, respectively, in the estimation of carbon storage. Myeong et al. (2004) developed a model with NDVI values obtained from Landsat ETM+ satellite imagery for the estimation of carbon storage in urban forests. This study showed that NDVI values can be used to estimate carbon stock (R^2=0.67). Situmorang et al. (2016) used vegetation indices to estimate carbon storage using NDVI and EVI, NDVI and EVI values were gathered from Landsat 8 OLI satellite image and models were developed to predict carbon storage using regression analysis. The coefficient (R^2) of the model developed with EVI was found to be 0.830, and the coefficient of the model developed with NDVI (R^2) was 0.728. Dos Reis et al. (2018) and Berra et al. (2012) tried to estimate the stand volume with the NDVI values obtained from the Landsat satellite image. In these studies, a significant correlation was found between the NDVI value and the stand volume (r=0.49 and r=0.61, respectively). Turgut and Günlü (2022) obtained reflectance, vegetation indices and texture values from Landsat 8 OLI satellite image to estimate aboveground biomass (AGB). The models were developed to predict AGB with multiple regression analysis (MLR). The adjusted coefficient of the models (R_a^2) developed with reflectance values, vegetation indices and texture values were found to be 0.445, 0.387 and 0.552, respectively. Ou et al. (2019) found a 91% correlation between the reflectance and vegetation indices values obtained from the Landsat 8 OLI satellite image and the AGB. Imran and Ahmed (2018) developed models to predict AGB using vegetation indices gathered from Landsat 8 OLI satellite imagery. One model was developed using SAVI (R^2=0.68) and other model developed using NDVI, DVI, ARVI, PVI and SAVI values together (R^2=0.63). Günlü and Ercanlı (2020) used ALOS PALSAR satellite imagery to estimate carbon storage in AGB in Göldağ planning unit. HH and HV polarizations, texture values and topographic information were obtained from ALOS PALSAR satellite image. Artificial neural networks (ANN) and MLR techniques were used. The HH and HV backscattering values and the model indication coefficients (R^2) with ANN were found to be 0.52 and 0.44, respectively, and 0.38, and 0.36 with the MLR. Keleş et al. (2021) estimated AGB by applying MLR, deep learning (DLM) and support vector machine (SVM) methods using remote sensing data obtained from

Sentinel-1 and Sentinel-2 satellite images in Scotch pine stands in Hızardere planning unit. The backscattering and polarization rates were obtained from Sentinel-1 satellite image, and reflectance and vegetation indices values were obtained from Sentinel-2. The fitted index (FI) of the model developed in the estimation of AGB with vegetation indices was found to be 0.531. Tavasoli et al. (2019) developed a model with SVM for the estimation of surface carbon stock with Sentinel-1, Sentinel-2, and ALOS PALSAR satellite images. The coefficients of the models developed with the help of ALOS PALSAR, Sentinel-1 and Sentinel-2 satellite images were determined as (R^2) 0.50, 0.60, and 0.51, respectively. Bolat (2019) used Göktürk-2 satellite imagery to estimate AGB and carbon stock in a Calabrian pine plantation stands. The success coefficient (R^2) of the model developed for biomass estimation with Göktürk-2 satellite imagery was found to be 0.50, while the coefficient (R^2) of the model developed for surface carbon stock was found to be 0.52. Askar et al. (2018) developed a model to predict AGB with the vegetation indices obtained from the Sentinel-2 (R^2=0.78). EVI and NDI values were included in this developed model. As a result of the literature review, our results were found to be compatible with the literature.

4. Conclusion

In this study, the relationship between NDVI acquired from Landsat 9 satellite image and AGC storage was calculated by regression analysis. A high positive correlation was found between NDVI values and AGC storage. The model developed for AGC storage prediction was moderate descriptive. The reasons for the moderate success of the developed model may be due to the low spatial resolution of the Landsat 9, the stand structure in the study area, topographic conditions and modeling technique. Therefore, using high-resolution satellite images with different modeling techniques (random forest, artificial neural networks, support vector machine, multivariate adaptive regression splines) for AGC prediction can increase model success. This study shows that the developed regression model can be useful for predicting AGC storage in pure Calabrian pine forests with similar forest ecosystems as our study area.

Acknowledgement

We would like to express our gratitude to the General Directorate of Forestry for providing the forest stand map and inventory data.

Conflict of interest

The authors declare that there is no conflict of interest.

References

Anand, A., Pandey, P. C., Petropoulos, G. P., Pavlides, A., Srivastava, P. K., Sharma, J. K., & Malhi, R. K. M. (2020). Use of Hyperion for Mangrove Forest Carbon Stock Assessment in Bhitarkanika Forest Reserve: A Contribution Towards Blue Carbon Initiative. *Remote Sensing*, *12*(4), 597. https://doi.org/10.3390/rs12040597

Askar, N. N., Phairuang, W., Wicaksono, P., & Sayektiningsih, T. (2018). Estimating Aboveground Biomass on Private Forest Using Sentinel-2 Imagery. *Journal of Sensors*, *2018*, 6745629. https://doi.org/10.1155/2018/6745629

Baniya, B., Tang, Q., Huang, Z., Sun, S., & Techato, K. A. (2018). Spatial and Temporal Variation of NDVI in Response to Climate Change and the Implication for Carbon Dynamics in Nepal. *Forests*, *9*(6), 329. https://doi.org/10.3390/f9060329

Beck, H. E., Zimmermann, N. E., McVicar, T. R., Vergopolan, N., Berg, A., & Wood, E. F. (2018). Present and Future Köppen-Geiger Climate Classification Maps at 1-km Resolution. *Scientific Data*, *5*(1), 180214. https://doi.org/10.1038/sdata.2018.214

Berra, E. F., Brandelero, C., Pereira, R. S., Sebem, E., Goergen, L. C. D. G., Benedetti, A. C. P., & Lippert, D. B. (2012). Total Wood Volume Estimation of *Eucalyptus* Species by Images of Landsat Satellite. *Ciência Florestal*, *22*(4), 853-864. https://doi.org/10.5902/198050987566

Bolat, N. (2019). *ÇAKÜ Orman Fakültesi Araştırma ve Uygulama Ormanında Göktürk-2 uydu görüntüsü kullanılarak topraküstü biyokütle ve karbon depolama miktarlarının belirlenmesi* [Master's thesis, Çankırı Karatekin University]. (in Turkish)

Bulut, S., Sivrikaya, F., & Günlü, A. (2022). Evaluating Statistical and Combine Method to Predict Stand Above-ground Biomass Using Remotely Sensed Data. *Arabian Journal of Geosciences*, *15*(9), 838. https://doi.org/10.1007/s12517-022-10140-3

Çepel, N. (2003). *Ekolojik sorunlar ve çözümleri*. TÜBİTAK. (in Turkish)

Chen, L., Ren, C., Zhang, B., Wang, Z., & Xi, Y. (2018). Estimation of Forest Above-ground Biomass by Geographically Weighted Regression and Machine Learning with Sentinel Imagery. *Forests*, *9*(10), 582. https://doi.org/10.3390/f9100582

Cusack, D. F., Axsen, J., Shwom, R., Hartzell-Nichols, L., White, S., & Mackey, K. R. (2014). An Interdisciplinary Assessment of Climate Engineering Strategies. *Frontiers in Ecology and the Environment*, *12*(5), 280-287. https://doi.org/10.1890/130030

Dos Reis, A. A., Carvalho, M. C., de Mello, J. M., Gomide, L. R., Ferraz Filho, A. C., & Acerbi Junior, F. W. (2018). Spatial Prediction of Basal Area and Volume in *Eucalyptus* Stands Using Landsat TM Data: An Assessment of Prediction Methods. *New Zealand Journal of Forestry Science*, *48*(1), 1. https://doi.org/10.1186/s40490-017-0108-0

Dvorakova, K., Heiden, U., Pepers, K., Staats, G., van Os, G., & van Wesemael, B. (2023). Improving soil Organic Carbon Predictions from a Sentinel–2 Soil Composite by Assessing Surface Conditions and Uncertainties. *Geoderma*, *429*, 116128. https://doi.org/10.1016/j.geoderma.2022.116128

Dvorakova, K., Shi, P., Limbourg, Q., & van Wesemael, B. (2020). Soil Organic Carbon Mapping from Remote Sensing: The Effect of Crop Residues. *Remote Sensing*, *12*(12), 1913. https://doi.org/10.3390/rs12121913

FMP (2022). *Forest management plans and inventory data of Burmahanyayla Planning Unit*. General Directorate of Forestry.

Gardin, L., Chiesi, M., Fibbi, L., & Maselli, F. (2021). Mapping Soil Organic Carbon in Tuscany through the Statistical Combination of Ground Observations with Ancillary and Remote Sensing Data. *Geoderma*, *404*, 115386. https://doi.org/10.1016/j.geoderma.2021.115386

Goodale, C. L., Apps, M. J., Birdsey, R. A., Field, C. B., Heath, L. S., Houghton, R. A., ... & Shvidenko, A. Z. (2002). Forest Carbon Sinks in the Northern Hemisphere. *Ecological Applications*, *12*(3), 891-899. https://doi.org/10.1890/1051-0761(2002)012[0891:FCSITN]2.0.CO;2

Gou, Y., Ryan, C. M., & Reiche, J. (2022). Large Area Aboveground Biomass and Carbon Stock Mapping in Woodlands in Mozambique with L-Band Radar: Improving Accuracy by Accounting for Soil Moisture Effects Using the Water Cloud Model. *Remote Sensing*, *14*(2), 404. https://doi.org/10.3390/rs14020404

Güner, Ş. T., Diamantopoulou, M. J., Poudel, K. P., Çömez, A., & Özçelik, R. (2022). Employing Artificial Neural Network for Effective Biomass Prediction: An Alternative Approach. *Computers and Electronics in Agriculture*, *192*, 1065960. https://doi.org/10.1016/j.compag.2021.106596

Günlü, A., & Ercanlı, İ. (2020). Artificial Neural Network Models by ALOS PALSAR Data for Aboveground Stand Carbon Predictions of Pure Beech Stands: A Case Study from Northern of Turkey. *Geocarto International*, *35*(1), 17-28. https://doi.org/10.1080/10106049.2018.1499817

Günlü, A., Ercanli, I., Başkent, E. Z., & Çakır, G. (2014). Estimating Aboveground Biomass Using Landsat TM Imagery: A Case Study of Anatolian Crimean Pine Forests in Turkey. *Annals of Forest Research*, *57*(2), 289-298. https://doi.org/10.15287/afr.2014.278

Günlü, A., Keleş, S., Ercanli, İ., & Şenyurt, M. (2021). Estimation of aboveground stand carbon using Landsat 8 OLI satellite ımage: A case study from Turkey. In P. K. Shit, H. R. Pourghasemi, P. Das, & G. S. Bhunia (Eds.), *Spatial Modeling in Forest Resources Management* (pp. 385-403). Springer, Cham.

Imran, A. B., & Ahmed, S. (2018). Potential of Landsat-8 Spectral Indices to Estimate Forest Biomass. *International Journal of Human Capital in Urban Management*, *3*(4), 303-314.

Jiang, F., Sun, H., Chen, E., Wang, T., Cao, Y., & Liu, Q. (2022). Above-ground Biomass Estimation for Coniferous Forests in Northern China Using Regression Kriging and Landsat 9 Images. *Remote Sensing*, *14*(22), 5734. https://doi.org/10.3390/rs14225734

Kahriman, A., Sönmez, T., Yavuz, M., Şahin, A., Yılmaz, S., Uzun, M., Kumaş, G., & Genç, Y. (2016). Antalya ve Mersin Yöresi Saf Kızılçam Meşcerelerinde Hasılat Araştırmaları, (TÜBİTAK-TOVAG, Project No: 112O808). (in Turkish)

Kauranne, T., Joshi, A., Gautam, B., Manandhar, U., Nepal, S., Peuhkurinen, J., Hämäläinen, J., Junttila, V., Gunia K., Latva-Käyrä, P., Kolesnikov, A., Tegel, K., & Leppänen, V. (2017). LiDAR-Assisted Multi-Source Program (LAMP) for Measuring Above Ground Biomass and Forest Carbon. *Remote Sensing*, *9*(2), 154. https://doi.org/10.3390/rs9020154

Keleş, S., Günlü, A., & Ercanli, İ. (2021). Estimating aboveground stand carbon by combining Sentinel-1 and Sentinel-2 satellite data: A case study from Turkey. In P. K. Shit, H. R. Pourghasemi, P. P. Adhikary, G. S. Bhunia, & V. P. Sati (Eds.), *Forest Resources Resilience and Conflicts* (pp. 117-126). Elsevier.

Labrecque, S., Fournier, R. A., Luther, J. E., & Piercey, D. (2006). A Comparison of Four Methods to Map Biomass from Landsat-TM and Inventory Data in Western Newfoundland. *Forest Ecology and Management*, *226*(1-3), 129-144. https://doi.org/10.1016/j.foreco.2006.01.030

Lal, R. (2008). Carbon Sequestration. *Philosophical Transactions of the Royal Society B: Biological Sciences*, *363*(1492), 815-830. https://doi.org/10.1098/rstb.2007.2185

Li, Y., Han, N., Li, X., Du, H., Mao, F., Cui, L., Liu, T., & Xing, L. (2018). Spatiotemporal Estimation of Bamboo Forest Aboveground Carbon Storage Based on Landsat Data in Zhejiang, China. *Remote Sensing*, *10*(6), 898. https://doi.org/10.3390/rs10060898

Myeong, S., Nowak, D. J., & Duggin, M. J. (2006). A Temporal Analysis of Urban Forest Carbon Storage

using remote sensing. *Remote Sensing of Environment*, *101*(2), 277-282. https://doi.org/10.1016/j.rse.2005.12.001

Nurda, N., Noguchi, R., & Ahamed, T. (2020). Forest Productivity and Carbon Stock Analysis from Vegetation Phenological Indices Using Satellite Remote Sensing in Indonesia. *Asia-Pacific Journal of Regional Science*, *4*(3), 657-690. https://doi.org/10.1007/s41685-020-00163-7

Ou, G., Li, C., Lv, Y., Wei, A., Xiong, H., Xu, H., & Wang, G. (2019). Improving Aboveground Biomass Estimation of *Pinus densata* Forests in Yunnan Using Landsat 8 Imagery by Incorporating Age Dummy Variable and Method Comparison. *Remote Sensing*, *11*(7), 738. https://doi.org/10.3390/rs11070738

Perry, E., Sheffield, K., Crawford, D., Akpa, S., Clancy, A., & Clark, R. (2022). Spatial and Temporal Biomass and Growth for Grain Crops Using NDVI Time Series. *Remote Sensing*, *14*(13), 3071. https://doi.org/10.3390/rs14133071

Pungpa, S., Chumkiew, S., & Piyatadsananon, P. (2023). Estimation of aboveground biomass and carbon stock using remote sensing data in Sakaerat Environmental Research Station, Thailand. In W. Boonpook, Z. Lin, P. Meksangsouy, & P. Wetchayont (Eds.) *Applied Geography and Geoinformatics for Sustainable Development* (pp. 207-215). Springer, Cham.

Saglam, S., Ozdemir, E., Ozkan, U. Y., Demirel, T., & Makineci, E. (2020). Biomass Estimation of Aboveground Tree Components for Turkey Oak (*Quercus cerris* L.) in South-eastern Turkey. *Environmental Monitoring and Assessment*, *192*(7), 418. https://doi.org/10.1007/s10661-020-08386-z

Sakici, O. E., Seki, M., & Saglam, F. (2018). Above-ground Biomass and Carbon Stock Equations for Crimean Pine Stands in Kastamonu Region of Turkey. *Fresenius Environmental Bulletin*, *27*(10), 7079-7089.

Situmorang, J. P., Sugianto, S., & Darusman, D. (2016). Estimation of Carbon Stock Stands Using EVI and NDVI Vegetation Index in Production Forest of Lembah Seulawah Sub-District, Aceh Indonesia. *Aceh International Journal of Science and Technology*, *5*(3), 126-139. https://dx.doi.org/10.13170/aijst.5.3.5836

Sivrikaya, F., & Bozali, N. (2012). Karbon Depolama Kapasitesinin Belirlenmesi: Türkoğlu Planlama Birimi Örneği. *Bartın Orman Fakültesi Dergisi*, *14*(1), 69-76. (in Turkish)

Sivrikaya, F., & Işık, M. (2022). Comparison of Biomass Estimation Approaches Based on Inventory Data: A Case Study in Kapıkaya Forest, Turkey. *Environmental Engineering & Management Journal*, *21*(5), 737-743.

Sivrikaya, F., Baskent, E. Z., & Bozali, N. (2013). Spatial Dynamics of Carbon Storage: A Case Study from Turkey. *Environmental Monitoring and Assessment*, *185*(11), 9403-9412. https://doi.org/10.1007/s10661-013-3260-x

Sivrikaya, F., Keleş, S., & Çakir, G. (2007). Spatial Distribution and Temporal Change of Carbon Storage in Timber Biomass of Two Different Forest Management Units. *Environmental Monitoring and Assessment*, *132*(1), 429-438. https://doi.org/10.1007/s10661-006-9545-6

Tavasoli, N., Arefi, H., Samiei-Esfahany, S., & Ronoud, Q. (2019). Modelling the Amount of Carbon Stock Using Remote Sensing in Urban Forest and Its Relationship with Land Use Change. *International Archives of the Photogrammetry, Remote Sensing & Spatial Information Sciences*, *42*(4), 1051-1058. https://doi.org/10.5194/isprs-archives-XLII-4-W18-1051-2019

Turgut, R., & Günlü, A. (2022). Estimating Aboveground Biomass Using Landsat 8 OLI Satellite Image in Pure Crimean Pine (*Pinus nigra* J.F. Arnold subsp. *pallasiana* (Lamb.) Holmboe) Stands: A Case from Turkey. *Geocarto International*, *37*(3), 720-734. https://doi.org/10.1080/10106049.2020.1737971

Wallis, C. I., Crofts, A. L., Inamdar, D., Arroyo-Mora, J. P., Kalacska, M., Laliberté, É., & Vellend, M. (2023). Remotely Sensed Carbon Content: The Role of Tree Composition and Tree Diversity. *Remote Sensing of Environment*, *284*, 113333. https://doi.org/10.1016/j.rse.2022.113333

Wang, S., Zhou, M., Zhuang, Q., & Guo, L. (2021). Prediction Potential of Remote Sensing-Related Variables in the Topsoil Organic Carbon Density of Liaohekou Coastal Wetlands, Northeast China. *Remote Sensing*, *13*(20), 4106. https://doi.org/10.3390/rs13204106

Wang, S., Zhuang, Q., Jin, X., Yang, Z., & Liu, H. (2020). Predicting Soil Organic Carbon and Soil Nitrogen Stocks in Topsoil of Forest Ecosystems in Northeastern China Using Remote Sensing Data. *Remote Sensing*, *12*(7), 1115. https://doi.org/10.3390/rs12071115

Wharton, E. H., & Griffith, D. M. (1993). *Methods to estimate total forest biomass for extensive forest inventories: Applications in the northeastern US*. US Department of Agriculture, Forest Service.

Xiao, J., Chevallier, F., Gomez, C., Guanter, L., Hicke, J. A., Huete, A. R., Ichii, K., Ni, W., Pang, Y., Rahman, A. F., Sun, G., Yuan, W., Zhang L., & Zhang, X. (2019). Remote Sensing of the Terrestrial Carbon Cycle: A Review of Advances over 50 Years. *Remote Sensing of Environment*, *233*, 111383. https://doi.org/10.1016/j.rse.2019.111383